УДК 621.039.553.5

ESTIMATION OF THE RADIATION ENVIRONMENT AND THE SHIELDING ASPECT FOR THE POINT2 AREA OF THE LHC*

*G.Shabratova, L.Leistam***

The estimation of the radiation environment for the POINT2 of the LHC, where it is planned to locate the ALICE detector, is presented. The dose level and neutron fluences have been studied in the FLUKA-95 and FLUKA-96 framework. The radiation levels have been investigated in the experimental cavern UX25 region, in the machine by-pass areas UL24, US25, UL26 and in the area of the counting rooms PX24. The radiation environment has been studied for two points of accidental beam losses. The dose level in the region of the counting rooms is lower than the recommended CERN limit 50mSv. The radiation level behind the access shielding at the air-duct chicane is not higher than 10mSv that is also appropriated for the use of this area as a public area. A more complicated situation is in the machine by-pass region UL24. The dose level in the tunnel is a few hundreds of mSv as a consequence of a rather small thickness of the separating wall between the shaft and the tunnel (near 1m). The decrease of the radiation level in this region could be achieved by increasing the wall or the beam pipe shielding thicknesses. The latter is more preferable as a cheaper variant.

The investigation has been performed at the Laboratory of High Energies, JINR.

Оценка радиационной обстановки в области пересечения2 LHC и аспекты защиты

Г.Шабратова, Л.Лейстам

Проведена оценка радиационной обстановки в районе пересечения 2 LHC, месте предполагаемого расположения экспериментальной установки ALICE. В рамках моделирующих пакетов FLUKA-95 и FLUKA-96 исследованы дозы радиации и нейтронные потоки. Эти характеристики определялись для экспериментальной зоны UX25, областей обводных машинных каналов UL24, US25, UL26 и района расположения измерительных комнат PX24. Аварийная высадка пучка на элементы вывода рассматривались как источник максимально возможной радиации. Радиационная обстановка была исследована для двух мест таких аварийных ситуаций. Найдено, что уровень доз в районе измерительных комнат не превышает установленного в ЦЕРНе допустимого предела 50 mSv. Уро-

*This work was supported by Engineering Support and Technologies Division of CERN under contract between European Laboratory for Particle Physics and Joint Institute for Nuclear Research.

**European Laboratory for Particle Physics, Geneva, Switzerland

вень радиации за защитой доступа, расположенной рядом с воздухопроводящим каналом области US25, не превышает 10 mSv, что позволяет использовать эту область для свободного доступа персонала. Более сложная ситуация наблюдается в туннеле канала UL24. Здесь доза составляет сотни mSv, что является следствием малой толщины стены, разделяющей шахту основного доступа и туннель. Снижение радиационного уровня в этой области может быть достигнуто увеличением толщины либо этой стены либо защиты, окружающей ионопровод вывода пучка. Последнее предпочтительнее как более дешевый вариант.

Работа выполнена в Лаборатории высоких энергий ОИЯИ.

1. Introduction

The nature of the world and, in particular, the structure of the matter have disturbed the inquisitive part of mankind for a long time. This curiosity initiates the preparation of more complicated and expensive experiments. Nowadays the scientific community hopes that some attractive ideas of high energy physics can be tested with the help of such an experimental facility as a multi-TeV collider. Among these hopes are the discovery of Higgs bosons in p–p interactions and the registration of Quark Gluon Plasma marks in nuclei-nuclei interactions. The creation of large Hadron Collider (LHC) in CERN can be considered as a next effort to provide the first look into the matter at mass scale of 1 TeV. But the operation of such collider at luminosities of $10^{34}\ \mathrm{cm}^{-2}\mathrm{s}^{-1}$ will be confronted by the radiation problems never met before. It is obvious that a thorough understanding of the radiation environment around experiments is required to guide the design of detectors and radiation shieldings.

The human safety is conditioned by the shielding strategy. The investigation of this strategy for the ion-ion experiment at LHC (ALICE) is the main task of the present report.

2. Machine Parameters

The main goal of the ALICE experiment is to study strongly interacting matter at extreme energy densities (QCD thermodynamics) which can be achieved in high-energy heavy-ion collisions. The scientific programme is based on the investigations of central collisions of such heavy nuclei like lead. In addition to the heavy (PbPb) system, the collaboration is planning to study the collisions of lower-mass ions and protons (both *pp*- and *p*-nucleus), which provide reference data for nucleus-nucleus collisions [1].

The LHC has been designed to be able to operate as a *proton-proton* and *ion-ion* collider. The energy per charge unit can be maintained at 7 TeV, giving for lead ions $E/A = 2.76$ TeV. The luminosity for these nuclei can reach $1.95 \times 10^{27}\ \mathrm{cm}^{-2}\mathrm{s}^{-1}$, i.e., almost seven orders of magnitude lower than for $p-p$ beams, $10^{34}\ \mathrm{cm}^{-2}\mathrm{s}^{-1}$ (see the table in Fig.2. with the LHC parameters recommended for radiation calculations [2,3].

The Pb-Pb cross section and average multiplicity are by factors of 35 and 200 larger than the *pp* ones and both factors decrease the difference between the *pp* and Pb-Pb radiation background up to three orders of magnitude. On the other hand the maximum

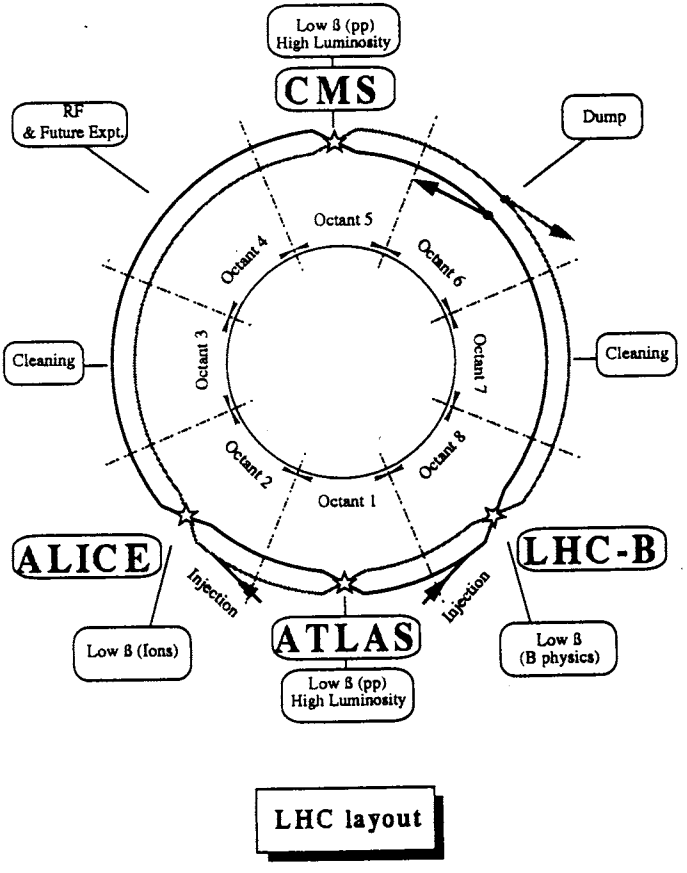

Fig.1. Layout of the LHC machine

Energy per charge E/Q	7 (TeV)
Energy per nucleon E/A	2.76 (TeV)
Peak luminosity L_{pp}	10^{34} ($cm^{-2}s^{-1}$)
PbPb luminosity L_{PbPb}	$(.85 - 1.95)\cdot 10^{27}$ ($cm^{-2}s^{-1}$)
Number of:	
protons per bunch N_b^{pp}	$4.7\cdot 10^{14}$
ions per bunch N_b^{ion}	$(6.3 - 9.4)\cdot 10^{7}$

Fig.2. The LHC parameters

luminosity of *proton-proton* collisions planned for use in the ALICE experiment is about 10^{30} $cm^{-3}s^{-1}$, that is four orders of magnitude lower than in the highest luminosity case, too.

These LHC parameters are very important to estimate a detector radiation load. But for the evaluation of the shielding [4] the accidental loss of a single proton beam is the limiting case.

3. Geometry of the ALICE Location Area

The LHC will be installed in the existing LEP tunnel after the decommisioning of LEP2. A schematic layout of the LHC is shown in Fig.1 [2].

The allocation of the ALICE is planned to be in the second octant of LHC in the region of the so-called Point2 (see Fig.1). This allocation is ideally suited for the detector. As the Point2 experimental area has been designed for the L3 experiment, no significant modifications will be needed for the experimental cavern or the surface zone. Two views of Point2 are shown in Fig.3 and Fig.4. The main access shaft, 23 m in diameter (PX24), has counting rooms. These rooms are separated from the experimental cavern 21.4 m in diameter (UX25) by a large concrete plug 2.4 m in thickness and a concrete screen 1.6 m thick (see Fig.3).

The more severe radiation environment of the LHC requires the reinforcement of the radiation shielding and a modification of a present access situation. A variant of this modification is presented in Fig.4. There are a concrete shielding 1.4 m in thickness

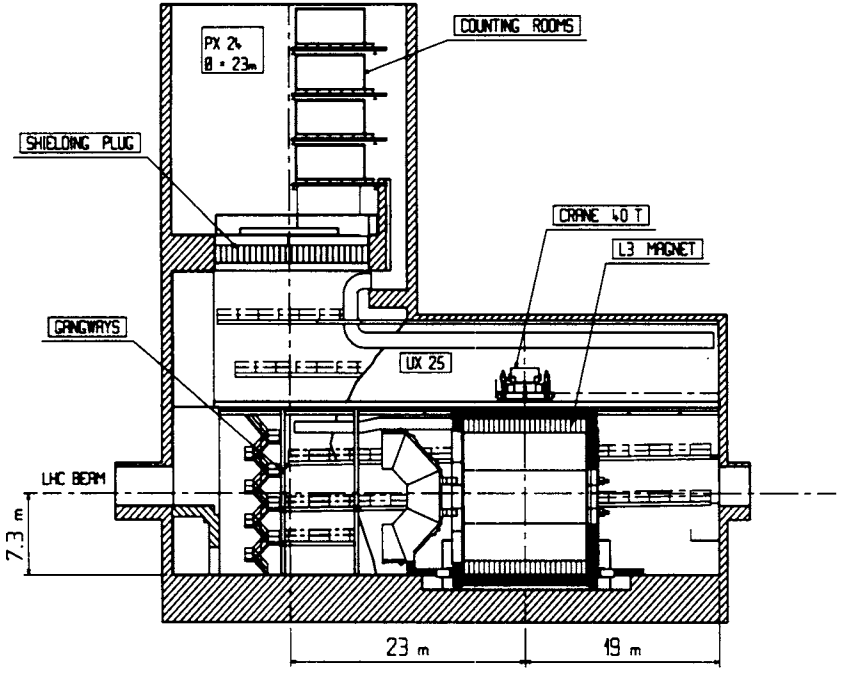

Fig.3. A *YZ* view of the access shaft and the experimental cavern

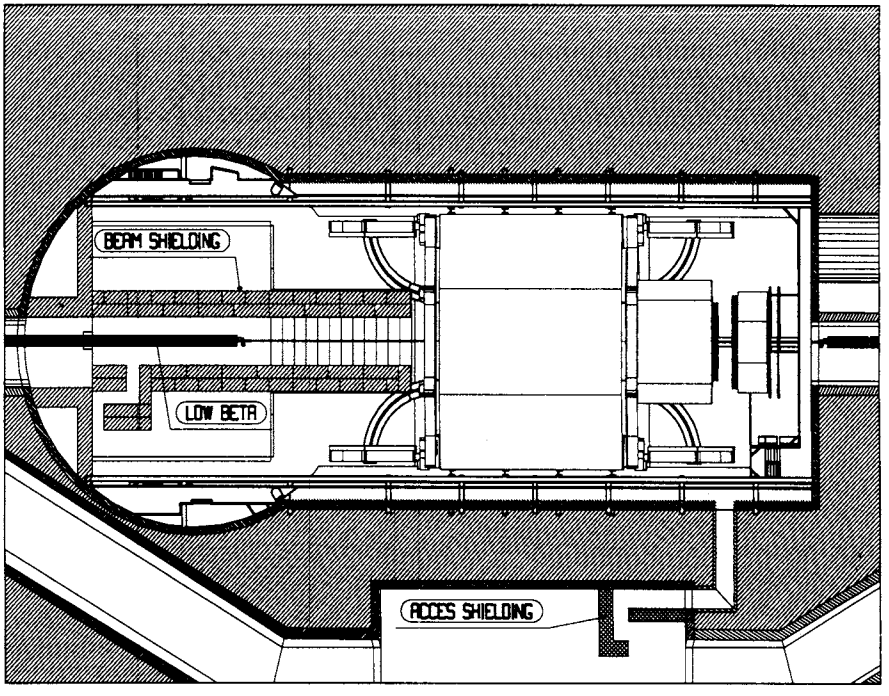

Fig.4. A *XZ* view of the experimental area and the machine by-pass region

surrounding the beam pipe section on the left side from the L3 magnet and concrete screens, called access shielding in Fig.4, at the air-duct chicane communicating the experimental area UX25 and the machine by-pass region (US25) in this modification.

In addition to the described regions there are two tunnels: a left tunnel in the UL24 area and a right one in the UL26 region in Fig.4.

4. Simulation Method

The multipurpose simulation tool named FLUKA (FLUctuating KAskade) [5,6] has been chosen as the most adequate model for the estimation of the radiation environment at LHC.

The cascade propagation through media is developed by this simulation package at a high accuracy level. In the FLUKA Monte-Carlo code [5] high energy interactions are simulated in the framework of the Dual Parton formalism [7]. Interactions at intermediate energies are treated by two distinct models: the resonance production and decay model covers an energy region (1.2-5.0) GeV and the sophisticated pre-equilibrium cascade is developed at energies below 1.3 GeV [8]. The evaporation module uses available nuclear mass and level density tabulations.

The Combinatorial Geometry package allows the accurate tracing of charged particles and Monte-Carlo transport calculations for neutrons and photons. The electromagnetic cascading is prepared by the EMF (Electro Magnetic Fluka) [6] where electrons, positrons and photons can be reliably transported to energies as low as 1-10 KeV. The neutron transport is based on multigroup transport theory using a 72 or 37 group structure [9] and is extended down to thermal energies.

A very accuracy multiple scattering algorithm [10] combined with magnetic field, the photoelectric effect, Compton and Rayleigh inelastic scattering, the pair production, bremsstrahlung, polarization and photonuclear interactions are taken into account in this simulating package.

The benchmark experiments [11,12] have shown that FLUKA is accurate within some tens of percent for dose and fluence estimation. For example, the energy and momentum are exactly conserved within the precision set by a computer (an internal check is set at 10^{-10}).

The important and unique feature of FLUKA is the possibility to use it as a fully analog code, in which case all correlations are presented, or to use any of powerfull variance reduction techniques that are essential for deep penetration studies. The latter can be applied to improve the convergence in some regions of phase space at the cost of others. There are available several techniques: region importance biasing, Russian roulette/splitting in hadronic interactions, leading particles biasing in electromagnetic interactions, non-analog absorption of low energy neutrons and decay length biasing [8].

4.1. *Simulation Conditions.* The geometry of Point2, shown in Figs.3 and 4 is described in terms of FLUKA Combinatorial Geometry. Only L3 magnet has been inserted into the FLUKA geomerty in order to maximize the radiation load of the investigated areas. The main geometric dimensions are shown in Figs.3,4. The sizes of the shielding plug and screen, thickness of the beam pipe shielding are quoted above. In addition to these values, the thickness of each access shielding is chosen to be equal to 80 cm. Thus the total number of volumes used in the FLUKA geometry is equal to 463, and the number of regions — to 995.

As the accidental loss of a single proton beam gives a maximum radiation load of the given regions in our case two points of the proton beam crash have been studied. It is considered in this investigation that only one bunch of $4.7 \cdot 10^{14}$ protons at 7000 GeV (see the table in Fig.2) can initiate such a crash of the LHC machine.

These points are:

— Point *A* is the bunch interaction at $z = -3035$ cm from the meet point of two beams with an iron target 1 m long and 2 cm in radius. This target was placed in the middle of the beam quadrupole;

— Point *B* is an analogous interaction point at $z = 2100$ cm.

The FLUKA95 and FLUKA96 codes were used to simulate the hadronic and electromagnetic cascades generated by primary bunch-target events. These events were simulated in the framework of the DTU JET generator inside the FLUKAS code.

The low limit of kinetic energy for the transport of all produced particles was equal to 10 MeV except antineutrinos and neutral kaons. Thier kinetic energy cut-off was 50 MeV.

The transport of the neutrons of the 72 group structure was switched on, but a detailed transport of electrons, positrons and photons (EMF) was not used. The latter could lead to

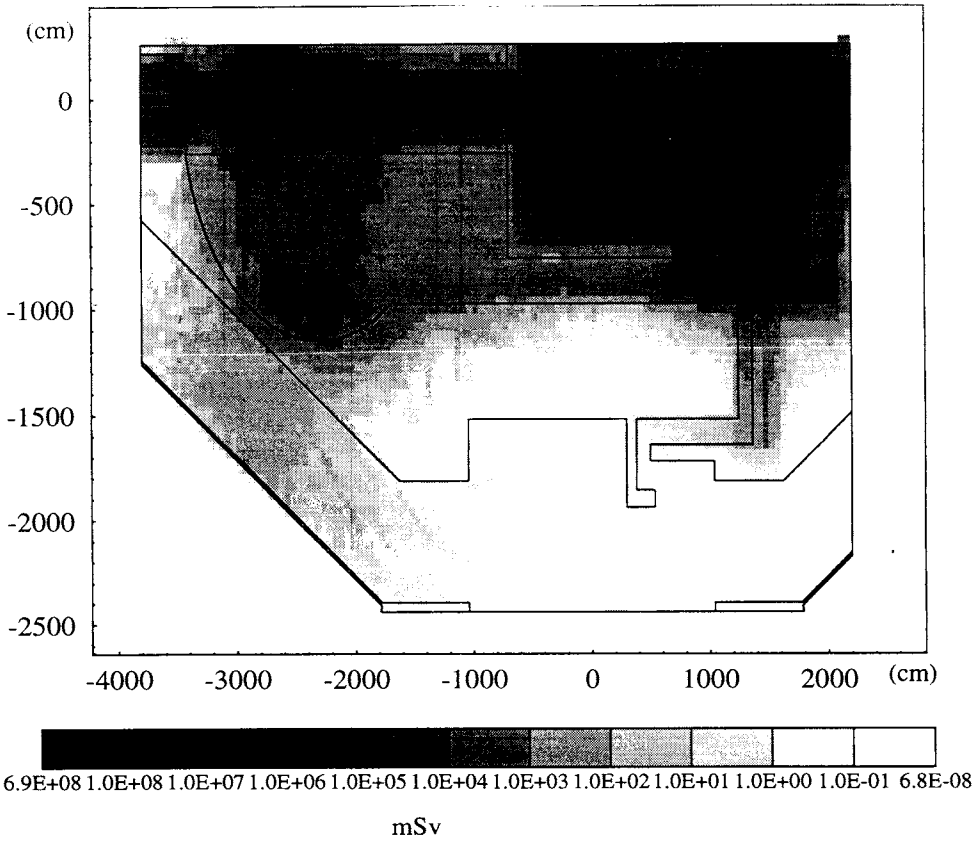

Fig.5. The dose level map for the point *A* in the *XZ* plane

a catastrophic CPU time as the FLUKA geometry of our sample has a huge number of regions mainly connected with dense media. On the other hand we are interested in the dose and neutron fluence in the regions far away from the interaction point, where main contributions are formed by charged hadron and neutron multiplication during their propagation through the matter.

The influence of the L3 magnet field (0.2 *T*) on a radiation load in the regions of our interest is rather weak, but switching on this field during the simulation could lead to a huge increase of the CPU time. For this reason we did not take into account the field of the L3 magnet.

In order to obtain statistically significant results in the investigated areas the following non-analog techniques were used: region importance biasing and Russian roulette/splitting in hadronic interactions. The volumes were divided into subregions or slices with different importance factors proportional to the hadronic mean free path for different regions. The importance increases in the direction of the investigated regions and decreases in the other directions.

The total energy deposition, neutron fluence and track-length were stored. As the main goal of this study is to understand the human safety aspect, the dose result should be

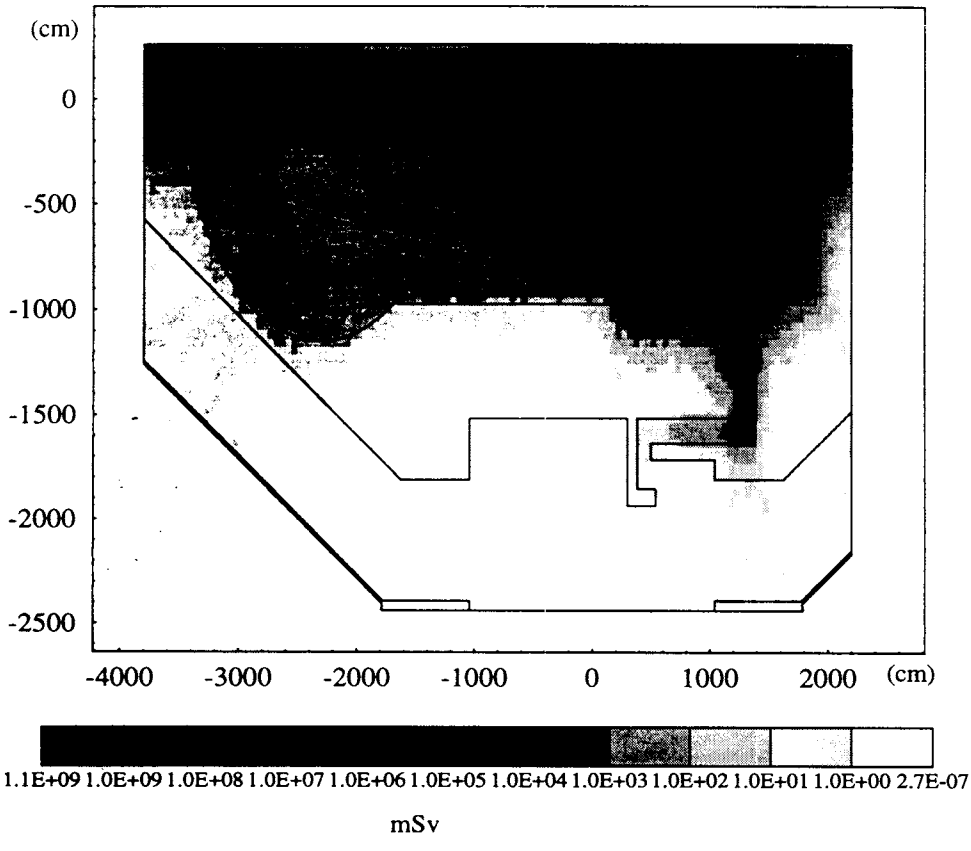

Fig.6. The dose level map for the point *B* in the *XZ* plane

presented in dose equivalent units of *Sv*. The dose equivalent is the absorbed dose weight by the quality factor which is adjusted to reproduce the damage caused in tissue by a given type of radiation. The track-length and energy deposition were weighed by the particle- and energy-dependent fluence to dose conversion factors [13,14].

5. Results

5.1. *Dose Levels.* The dose maps in the *XZ* plane for both points *A* and *B* can be found in Figs.5 and 6.

We shall analyse the radiation environment in the public areas, only.

The most serious situation is observed for the UL24 tunnel. Here the dose level is high as a sequence of rather a small thickness of the separating wall between the shaft and the tunnel (near 1 m). Fig.7 presents a zoom picture of the dose level in this region and Fig.8 shows the dose as a function of the shaft sideway distance inside the UL24 tunnel. It is

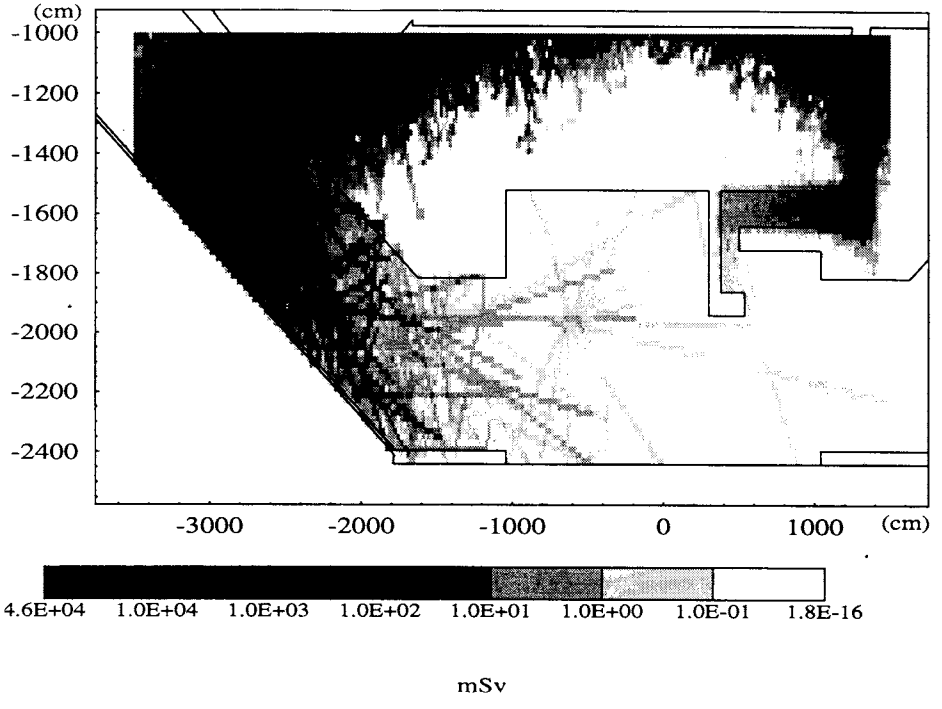

Fig.7. The zoom of the dose level map for point *A*

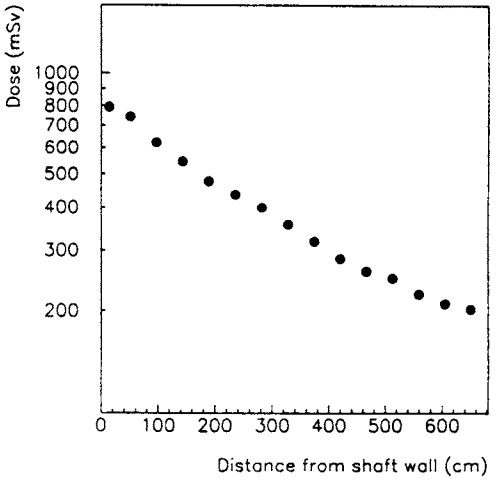

Fig.8. The dose as a function of the shaft sideway distance inside the UL24 tunnel

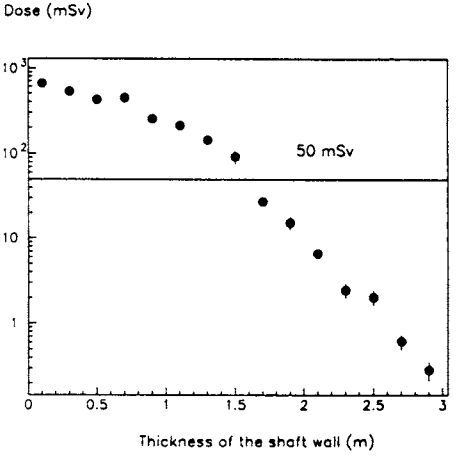

Fig.9. The dependence of the dose on the thickness of the shaft wall at a beam shielding of 2.4 m

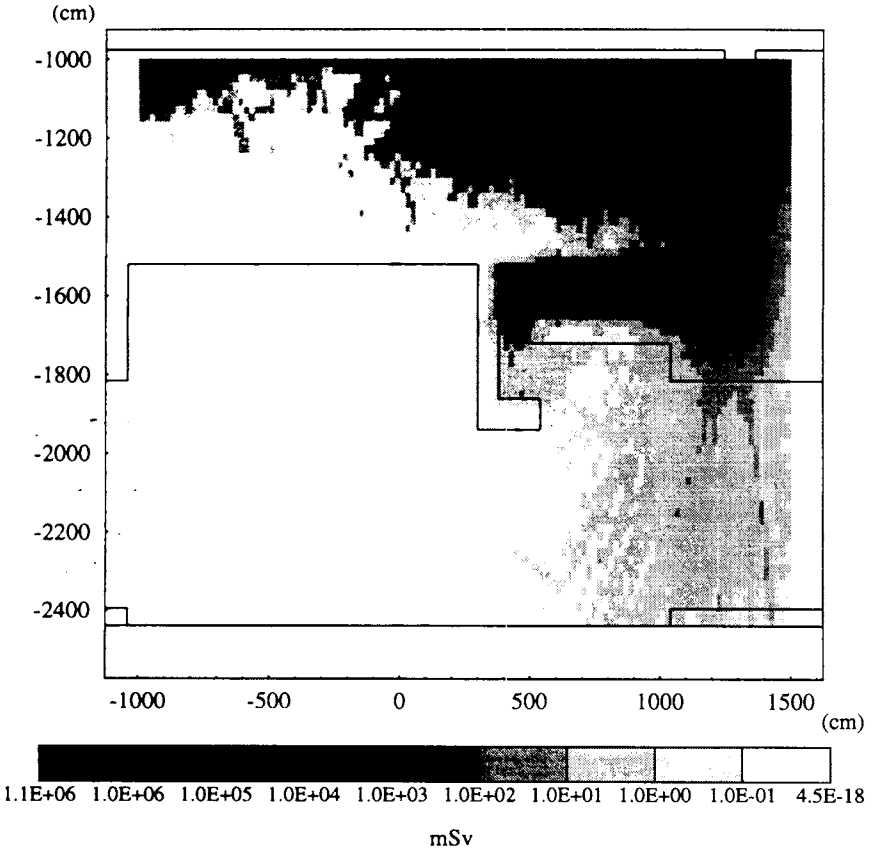

Fig.10. The dose level map for the air-duct chicane region at point *B* in the *XZ* plane

rather a high dose level, which is equal to a few hundreds of mSv in the tunnel. At the point very close to the shaft wall, the dose is a little bit smaller than a thousand mSv. In our earlier report [15], we have shown that a softer situation could be attained by increasing the beam shielding thickness, see Fig.9, where a dose-depth dependence for an infinite wall thichness is presented at a beam shielding thickness of 2.3 m.

The radiation load in the US25 air-duct chicane region behind access shielding is roughly the same for both points (*A* and *B*) and does not exceed 10 mSv. The zoom picture for point *B* is presented in Fig.10. It is obvious, that this area could be used as a public area because the dose is lower than recommended CERN safety limit equal to 50 mSv.

It is seen from Figs.5,6 that the most serious radiation load in the shaft region is observed for point *A*. The dose level in this area is roughly ten times higher than for point *B* case.

Following this conclusion, we present the dose level map in the *XZ* plane only for point *A* in Fig.11. A zoom picture of the area of the most interest, the region of the counting rooms, is depicted in Fig.12. The dose dependences on the plug surface distance for it are

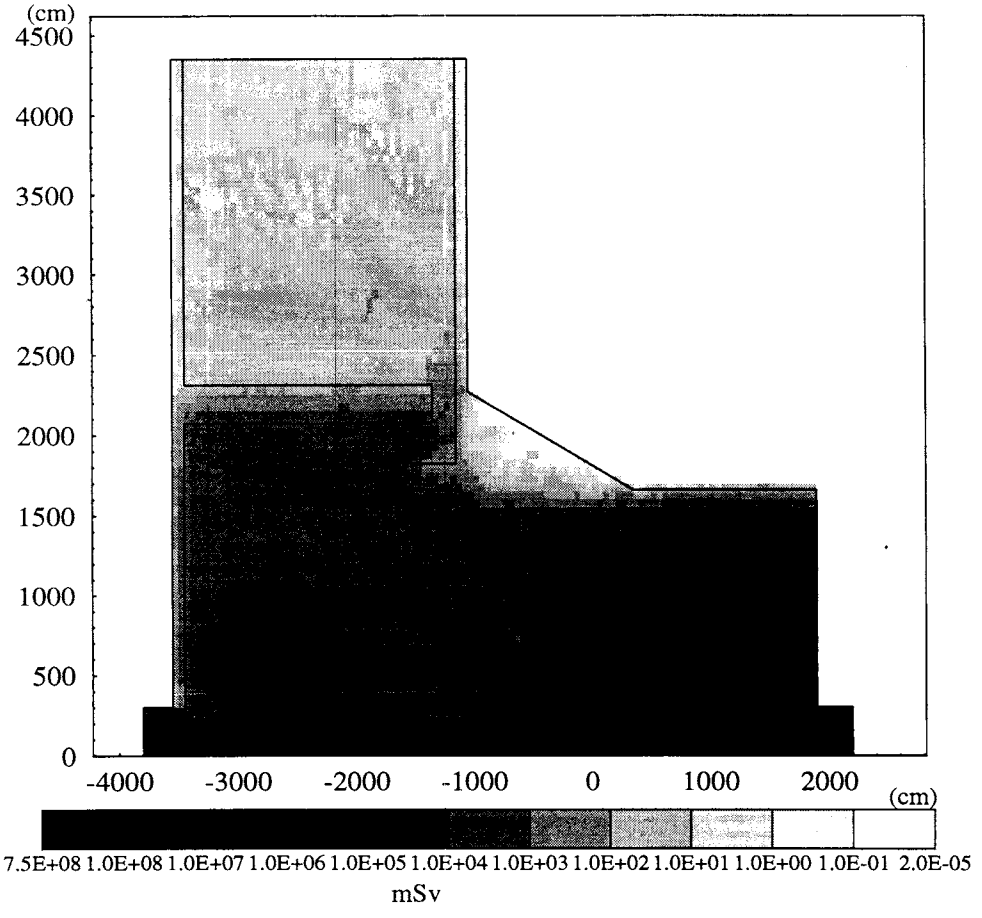

Fig.11. The dose level map for point *A* in the *YZ* plane

in Fig.13. The dependence for the area above the plug is in Fig.13(a) and for the region above the air-duct chicane is in Fig.13(b). It is seen that the dose level in the area of the counting rooms does not exceed the recommended CERN limit, except the regions very close to the chicane. The additional shielding perpendicular to the plug surface (Fig.3) would have to decrease the dose level in this area to a safety level of 50 mSv.

5.2. *Neutron Fluences.* The fluence maps of the neutrons with kinetic energies greater than 100 KeV are shown in Figs.14—16.

The *YZ* view (Fig.14) is given only for point *A* as a map with a greater neutron load. One can see that neutron fluence in the region of the counting rooms does not exceed 10^{12} neutrons per cm^2.

The *XZ* views (Figs.15—16) are presented for the regions of the most interest. The maximum fluence observed in the UL24 tunnel for point *A* (Fig.15) is about $5.0 \cdot 10^{12}$

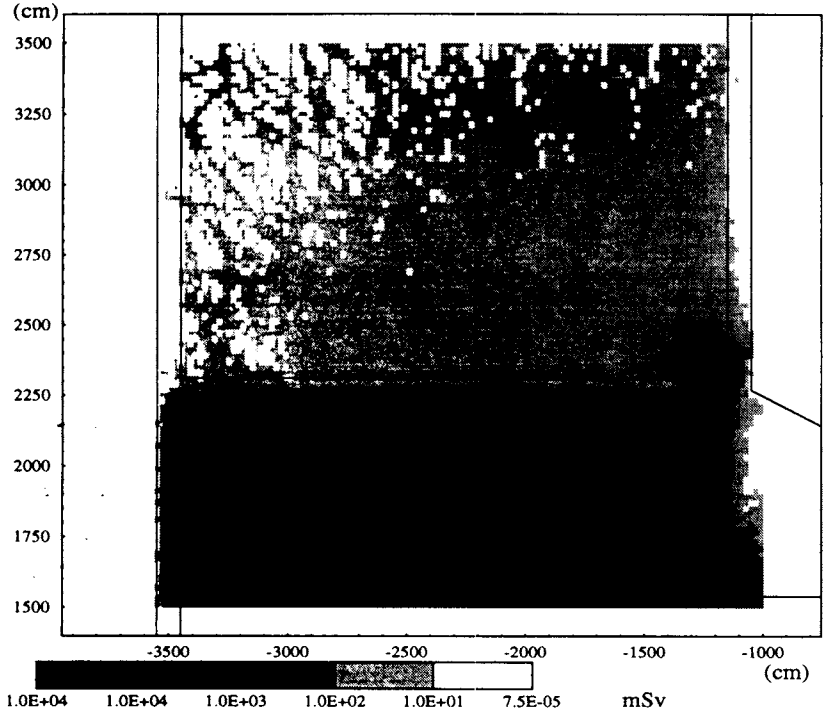

Fig.12. The dose level map in the region of the counting rooms point *A*

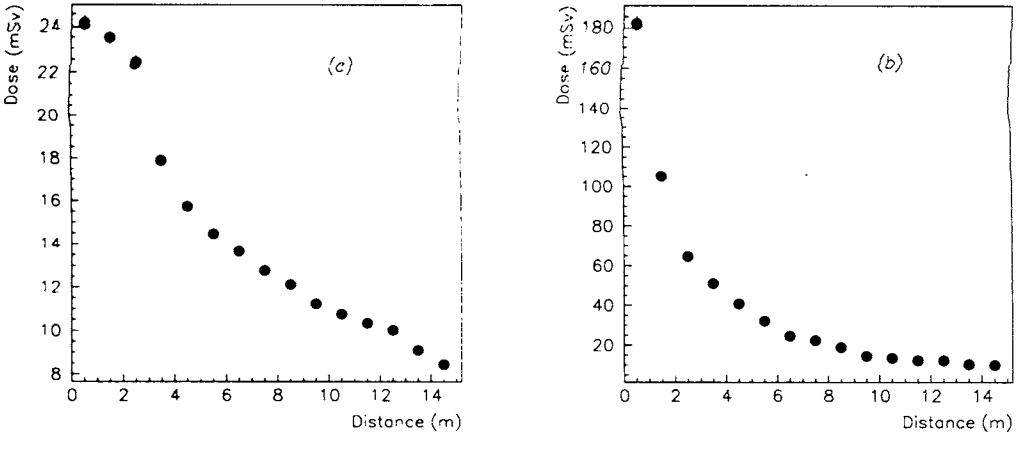

Fig.13. The dose-depth dependence in the counting room area (a) — in the area above the plug surface, (b) — above the air-duct chicane

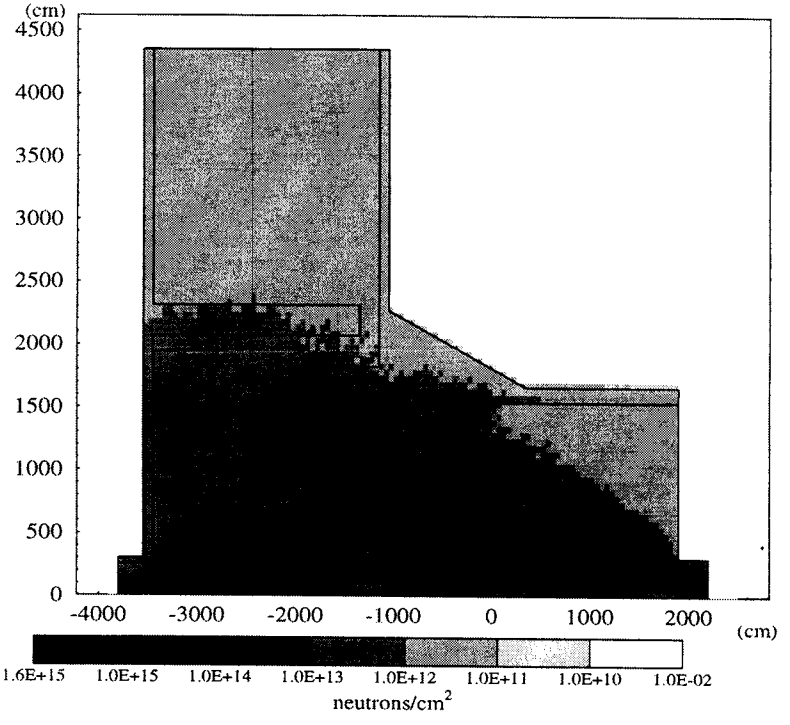

Fig.14. The neutron fluence map for point *A* in the *YZ* plane

neutrons per cm^2. The public area behind the access shielding in the UX25 region for point *B* (Fig.16) has neutron load per cm^2 a little bit greater than 10^{12}.

6. Conclusion

1. It has been found that the dose level in the region of the counting rooms PX24 does not exceed the recommended CERN limit.

2. The radiation level behind the US25 access shielding at the air-duct chicane is not higher than 10 mSv that is also appropriated for the use of this area as a public area.

3. A more complicated situation is in the machine by-pass region of the UL24 tunnel. The dose level in this region is a few hundreds of mSv. The decrease of the radiation load in this region could be achieved by increasing the shaft wall or the beam pipe shielding thickness. The latter is more preferable as a cheaper variant.

4. The fluences of neutron at kinetic energy greater 100 KeV in the public areas do not exceed 10^{13} neutrons per cm^2.

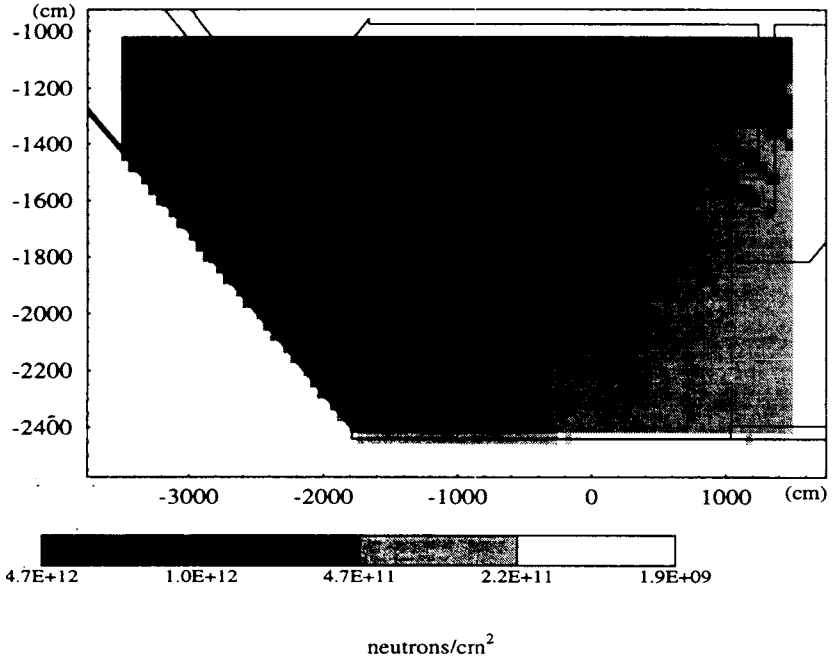

Fig.15. The neutron fluence map for the machine by-pass region, point *A*

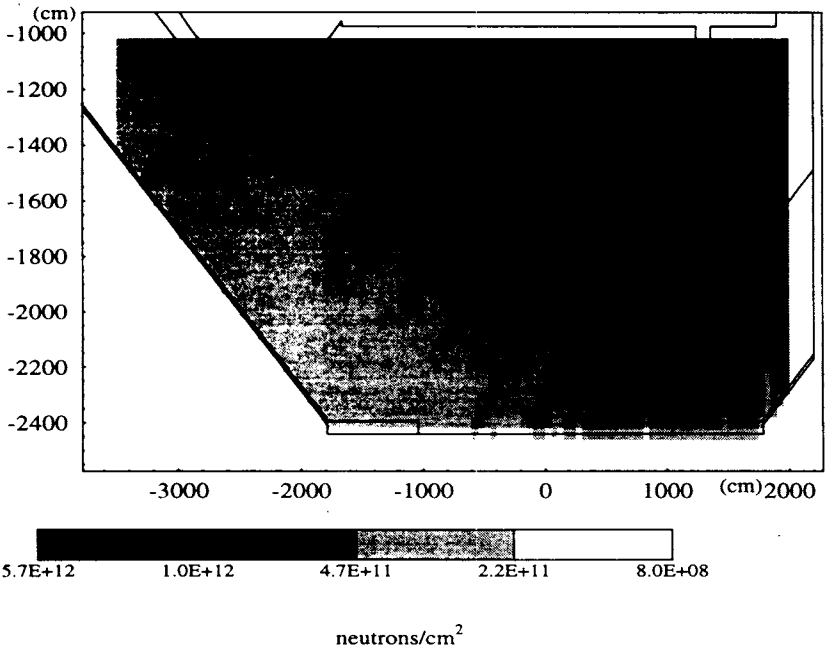

Fig.16. The neutron fluence map for the machine by-pass region, point *B*

Acknowledgements

We would like to thank M.Huhtinen, K.Potter, S.Rollet and G.Stevenson for their help and prolific discussions, A.Vodopianov for constant interest in this work.

References

1. ALICE TP CERN/LHCC 95-71 LHCC/P3.
2. The LHC Study Group, The Large Hadron Collider, Conceptual Design, CERN/AC/95-05(LHC), ed. P.Lefevre and T.Petterson (1995).
3. Hofert M., Potter K., Stevenson G. — CERN/TIS-RP/IR/95-19 (1995).
   Potter K., Stevenson G. — CERN/TIS-RP/IR/95-05.
   Potter K., Stevenson G. — CERN/TIS-RP/IR/95-11.
   Potter K., Stevenson G. — CERN/TIS-RP/IR/95-16.
4. Stevenson G., Hoefert M. — CERN/TIS-RP/IR/94-18.
5. Fasso A., Ferrari A., Ranft J., Sala P.R. — Proc. IV Int. Conf. on Calorimetry in High Energy Physics, La Biodola (Is. d'Elba), Sep. 20—25 1993, ed. A.Menzione and A.Scribano, World Scientific, p.493.
6. Aarnio P. et al. — MC93 Int. Conf. on Monte Carlo Simulation in High Energy and Nuclear Physics, p.88, ed. P.Dragowitscj, S.Linn and M.Burbank, World Scientific, 1994.
7. Capella A., Tran Thanh Van J. — Phys. Lett., 1980, v.93B, p.146.
8. Fasso A., Ferrari A., Ranft J., Sala P. — Specialists' Meeting on Shielding Aspects of Accelerators, Target and Irradiation Facilities, Arlington, Texas, April 28—20, 1994.
9. Ferrari A., Sala P., R.Guaraldi R., Padoani F. — Nucl. Instr. and Meth., 1992, v.B71, p.412.
10. Ferrari A., Sala P. —Nucl. Instr. and Meth., 1992, v.B71, p.412.
11. Fasso A. et al. — Nucl. Instr. and Meth., 1993, v.A332, p.459.
12. Birattari C. et al. — Nucl. Instr. and Meth., 1994, v.A338, p.534.
13. IRCU Report 40 (1986) and ICRP Publication 60, Pergamon Press (1991).
14. Sannikov A.V., Savitskaya E.N. — CERN/TIS-RP/93-14 (1993).
15. Chabratova G., Klempt W., Leistam L., Slavin N. — ALICE/95/41, Internal Note.

Received on April 18, 1997.